

Numerical renormalization group of vortex aggregation in 2D decaying turbulence: the role of three-body interactions

Clément Sire and Pierre-Henri Chavanis

Laboratoire de Physique Quantique (UMR C5626 du CNRS), Université Paul Sabatier

31062 Toulouse Cedex, France.

(clement@irsamc2.ups-tlse.fr & chavanis@irsamc2.ups-tlse.fr)

(Version of April 26, 2024)

Abstract

In this paper, we introduce a numerical renormalization group procedure which permits long-time simulations of vortex dynamics and coalescence in a 2D turbulent decaying fluid. The number of vortices decreases as $N \sim t^{-\xi}$, with $\xi \approx 1$ instead of the value $\xi = 4/3$ predicted by a naïve kinetic theory. For short time, we find an effective exponent $\xi \approx 0.7$ consistent with previous simulations and experiments. We show that the mean square displacement of surviving vortices grows as $\langle x^2 \rangle \sim t^{1+\xi/2}$. Introducing effective dynamics for two-body and three-body collisions, we justify that only the latter become relevant at small vortex area coverage. A kinetic theory consistent with this mechanism leads to $\xi = 1$. We find that the theoretical relations between kinetic parameters are all in good agreement with experiments.

PACS numbers: 47.10.+g, 47.27.-i

I. INTRODUCTION

In recent years, a great deal of work has been devoted to the study of two-dimensional turbulence. Two-dimensional turbulence is not only relevant to the study of geophysical and astrophysical flows, but it is also far more accessible to modern computers and experiments, since the measurement and the visualization of the velocity and vorticity fields are much easier than in $D = 3$. In addition, two-dimensional turbulence has deep connections with other fields of physics such as electron plasmas in magnetic field [1] and stellar dynamics [2].

For the specific problem of two-dimensional decaying turbulence, recent experimental [3–5] and theoretical [6–16] works have emphasized the importance of coherent vortex dynamics during the fluid decay. This process essentially consists in three stages: during an initial transient period, the fluid self-organizes and a network of coherent vortices appears. Once the coherent vortices have emerged, vortices disappear through mergings of like-sign vortices, such that their number N decreases and their average radius r increases, in a process somewhat reminiscent of a coarsening dynamics [16]. During this process, and in the limit of small viscosity, energy remains constant. When only one dipole (or very few) remains, it finally decays diffusively.

From the theoretical point of view, the “coarsening” stage is certainly the most interesting as, in principle, it can extend on an arbitrary long time period. In this regime, the main question arising concerns the existence of universal features including the decay exponent ξ ($N \sim t^{-\xi}$), and other exponents which describe the time evolution of quantities such as the average vortex radius, the enstrophy or the kurtosis.

In this paper, we first describe an effective model for the vortex dynamics and review the main experimental and numerical results concerning the temporal evolution of the physical quantities listed above. In section **II**, we show that the surviving vortices have a hyperdiffusive motion with an effective diffusion coefficient $D \sim t^{\xi/2}$, and a flight time distribution behaving as $P(\tau) \sim \tau^{\xi/2-3}$. We then consider a “naïve” kinetic theory for the vortex decay dynamics predicting $\xi = 4/3$. In section **III**, we introduce a numerical renormalization group (RG) procedure which permits very long simulation times. Although the numerical diffusion coefficient is well described by the preceding kinetic theory, the decay exponent is found to be significantly lower than expected ($\xi \approx 1$ instead of $\xi = 4/3$). In section **IV**, we derive an effective dynamics for 2 and for 3 neighboring vortices subjected to the effective noise due to far away vortices. Within these simple models, we relate the average merging time to the decay exponent ξ found in the RG simulations. Our main conclusion is that the lower than expected value for ξ could be explained by the fact that two-body collisions are irrelevant at large time, whereas three-body collisions predominate. In section **V**, we present a simple kinetic theory taking these three-body collisions into account and yielding $\xi = 1$. The importance of three-body collisions in vortex dynamics was previously pointed out by Novikov [17], in a different context. Throughout this paper, we compare our results to recent experiments [3–5] and find a very good overall agreement.

II. KIRCHHOFF MODEL

A. Generalities

As we are mainly concerned with the coherent vortex dynamics and merging processes, it is natural to focus on the effective behavior of the sole vortices, neglecting the incoherent background.

The route to such an effective model starts with the work of Kirchhoff [18] who obtained the equations of motion of point-like vortices in the zero viscosity limit. Vortices follow a Hamiltonian dynamics where the vortex center coordinates x_i and y_i are conjugate variables:

$$\Gamma_i \frac{dx_i}{dt} = \frac{\partial H}{\partial y_i}, \quad (1)$$

$$\Gamma_i \frac{dy_i}{dt} = -\frac{\partial H}{\partial x_i}, \quad (2)$$

where Γ_i is the circulation of vortex i , and where H denotes the following Hamiltonian:

$$H = -\sum_{i \neq j} \Gamma_i \Gamma_j \ln(r_{ij}), \quad (3)$$

where r_{ij} stands for the distance between vortices i and j . These equations of motion can be more explicitly written:

$$\frac{dx_i}{dt} = -\sum_{j \neq i} \Gamma_j \frac{y_{ij}}{r_{ij}^2}, \quad (4)$$

$$\frac{dy_i}{dt} = \sum_{j \neq i} \Gamma_j \frac{x_{ij}}{r_{ij}^2}. \quad (5)$$

These equations are strictly valid for point-like vortices and cannot describe vortex mergings. This should be accounted by hand by defining *ad hoc* merging rules as introduced in [7,9,13]. The authors of [9] determined a criterion for the merging of two like-sign vortices of radii r_1 and r_2 , within the elliptical-moment model [19]. They found that, for $r_1 \leq r_2$, collapse can be observed for an initial vortex separation $d < r_c = ar_2 + br_1^2/r_2$, where a and b are numerical constant of order 1 ($a \approx 2.59$, $b \approx 0.61$ [9]). Using $r_1 < r_2$ and $a > 3b$, one easily obtains

$$\frac{a+b}{2}(r_1 + r_2) \leq r_c \leq a(r_1 + r_2), \quad (6)$$

which shows that r_c is of the order of the mean radius. In [13], the authors in fact used $r_c = a'(r_1 + r_2)$ ($a' \approx 1.7$). Thus, if one considers a collection of vortices of the same typical size, it is clear that choosing the same critical distance for all mergings, equal to the average radius r of the population of vortices, cannot drastically affect the model properties. This was actually verified in [16]. Now that the merging criterion has been given, the properties of the vortex resulting from the merging of two like-sign vortices must be specified. Motivated by experiments [3–5] and numerical simulations [9,12,13], the authors of [12,13] and [7,9] assumed that the average peak vorticity ω is conserved throughout the merging process, as well as the energy since the inviscid limit is considered. As the total energy scales as $E \sim N\omega^2 r^4$ (with a possible $\ln N$ correction), this shows that Nr^4 should be conserved,

or equivalently that a vortex of radius $r' = (r_1^4 + r_2^4)^{1/4}$ results from the merging of two vortices of radii r_1 and r_2 . Note that this conservation law is consistent with the observed slow enstrophy dissipation [12].

Numerical simulations of this model starting from a population of vortices having the same typical radius results in a narrow radius distribution at all subsequent times [9,16]. Moreover, it is observed that the number of vortices decays as a power law

$$N(t) \sim \frac{N_0}{(1 + t/t_0)^\xi}, \quad (7)$$

with $\xi \approx 0.70 - 0.75$, much smaller than the exponent predicted by Batchelor theory ($\xi = 2$) [20]. The conservation of the total energy and mean peak vorticity leads to the occurrence of only one independent exponent for the time evolution of physical quantities [7,9]:

$$N(t) \sim R^{-2} \sim t^{-\xi}, \quad r \sim t^{\xi/4}, \quad (8)$$

$$Z \sim t^{-\xi/2}, \quad K \sim t^{\xi/2}, \quad (9)$$

where R is the typical distance between vortices, and Z and K are respectively the enstrophy and the kurtosis.

The exponent ξ and the predicted scaling laws are consistent with experiments [3–5] and direct numerical simulations [9] of Navier-Stokes (NS) equation (using a hyperviscous dissipation term).

B. Limitation of numerical simulations

The Kirchoff simulations and actual experiments cited above were only carried out for very short time. In [9] (as well as in experiments [3–5]), the number of vortices decays by less than a factor 4 at the maximal accessible time t_{\max} . Raw data show significant curvature on a log-log plot, hence the introduction of an extra fitting parameter t_0 in [9] (see Eq. (7)). Since $t_0 \approx t_{\max}/3$, the simulation time is of the order of the transient time t_0 , and the scaling regime for $t \gg t_0$ is probably not reached. As a matter of fact, the actual exponent ξ obtained by measuring the logarithmic slope at the final time is of order $\xi \approx 0.6$, as obtained by Benzi and co-workers [13,14] (see also section **III.B**)

It would be interesting to explore the domain of lower vortex density n , as in all simulations performed so far the mean free path (of the order of the typical distance between vortices [11,21]) remains of the same order as the radius size. In other words, the fraction of area occupied by the vortices,

$$s = \frac{N\pi r^2}{L^2} = n\pi r^2 = \pi \left(\frac{r}{R}\right)^2, \quad (10)$$

remains quite large in the early time of the dynamics. Because of the scaling laws of Eq. (8), R grows faster than the mean radius r , such that vortices become effectively more and more point-like, a regime which seems to be out of numerical reach, and which should develop for $t \gg t_0$.

C. Kinetic theory for the Kirchhoff model

1. Diffusion coefficient

In the absence of mergings, the chaotic Kirchhoff dynamics is known to lead to an effective diffusive motion of the vortices [16,11,21]. The diffusion coefficient can be calculated by computing the fluctuation time $T(v)$ for a given vortex velocity v and averaging the quantity $v^2 T(v)/4$ over the velocity distribution. This calculation has been extensively described in [21] and we present here a simple heuristic argument leading more directly to the same result.

Using Eq. (4) and Eq. (5), the average velocity squared is

$$\langle v^2 \rangle \sim \sum_j \frac{\Gamma_j^2}{r_{ij}^2}, \quad (11)$$

where we have neglected the contribution of off-diagonal terms obtained when squaring Eq. (4) and Eq. (5). If we assume the vortices to be uniformly distributed on average, and the circulations to be equal up to their sign, we then obtain

$$\langle v^2 \rangle \sim N\Gamma^2 \frac{2}{L^2} \int_r^L \frac{x dx}{x^2} \sim 2n\Gamma^2 \ln(L/r) \sim n\Gamma^2 \ln N, \quad (12)$$

where we have introduced the vortex typical radius r as a natural cut-off. This expression already obtained in [16] has been qualitatively checked in [11] and is confirmed by our simulations of section **III.B**.

It is then natural to assume that the mean free path l is of order R , the typical distance between vortices, as proved in [21]. We then get the expressions for the mean free time τ and the diffusion coefficient:

$$l \sim R, \quad \tau \sim \frac{l}{v} \sim (n\Gamma\sqrt{\ln N})^{-1}, \quad D \sim \frac{l^2}{\tau} \sim \Gamma\sqrt{\ln N}, \quad (13)$$

in agreement with our more sophisticated treatment [21].

Now, if we include merging events, these different quantities are expected to vary with time as both the density n and the typical circulation Γ do. If we drop logarithmic corrections for now, we obtain

$$l \sim t^{\xi/2}, \quad \tau \sim t^{\xi/2}, \quad v \sim \text{const.}, \quad D \sim t^{\xi/2}. \quad (14)$$

Note that this expression for the diffusion coefficient D differs from that obtained in [5] ($D \sim t^{3\xi/4}$). Indeed, the authors of [5] used the merging time $\tau_{\text{merg.}}$ to compute D , instead of the fluctuation or mean free time which is relevant here [21,11]. A naïve estimate of this merging time is addressed in the next subsection.

Finally, we predict that the mean square displacement of surviving vortices (or test particles) in the decaying fluid should behave as [21]

$$\langle x^2 \rangle \sim t^\nu, \quad \text{with} \quad \nu = 1 + \frac{\xi}{2}. \quad (15)$$

In [5], the authors found $\xi \approx 0.7$, which leads to $\nu \approx 1.35$, using Eq. (15). This must be compared with the experimental value $\nu \approx 1.3$ for vortices and $\nu \approx 1.4$ for test particles moving along the current lines of the fluid. Eq. (15) is also in good agreement with our simulations of section **III.B**.

Note that this hyperdiffusive behavior can be interpreted by invoking a power-law decreasing flight time distribution (time between two deflections or large velocity fluctuations). Let us assume that this distribution behaves as

$$P(\tau) \sim \tau^{-\mu}, \quad \text{for } \tau \rightarrow +\infty, \quad (16)$$

with $\mu > 2$, such that the average fluctuation time exists. Then, after a time $t = \sum_{i=1}^m \tau_i \sim m\langle\tau\rangle$ (m deflections), and using that $\langle v^2 \rangle$ is essentially constant, the mean square displacement reads

$$\langle x^2 \rangle \sim \langle v^2 \rangle \left\langle \sum_{i=1}^m \tau_i^2 \right\rangle \sim m \int^t \tau^{2-\mu} d\tau \sim t^{4-\mu}. \quad (17)$$

This shows that within this interpretation $\nu = 4 - \mu$, or

$$\mu = 3 - \frac{\xi}{2}. \quad (18)$$

Using $\xi \approx 0.7$, we find $\mu \approx 2.65$, in good agreement with the experimental value $\mu = 2.6 \pm 0.2$ measured in [5].

2. Naïve kinetic theory

The merging time $\tau_{\text{merg.}}$ is the typical time between two merging events involving the same vortex. If we assume that vortex mergings occur whenever two like-sign vortices stand at a distance less than $r_c \sim r$, a classical cross-section argument leads to

$$\tau_{\text{merg.}} \sim (nvr)^{-1}. \quad (19)$$

If we assume a scaling regime where $n(t)$ decays as a power law, $\tau_{\text{merg.}}$ must behave linearly with time [22] as

$$\frac{dn}{dt} \sim -\xi \frac{n}{t} \sim -\frac{n}{2\tau_{\text{merg.}}}. \quad (20)$$

Using the scaling equations Eq. (8) and Eq. (14), and the above expression for $\tau_{\text{merg.}}$, we finally obtain

$$\tau_{\text{merg.}} \sim v^{-1} t^{\frac{3}{4}\xi} \sim t^{\frac{3}{4}\xi}, \quad (21)$$

neglecting logarithmic corrections in v . The constraint $\tau_{\text{merg.}} \sim t$ then leads to $\xi = 4/3$, well above the measured value $\xi \approx 0.7$. Note that our argument is fully consistent with a direct simulation performed by Trizac [22], who found $\xi \approx 0.7$, in a ballistic system obeying the same conservation laws as in the vortex model, but for which the typical velocity decreases

as $v \sim t^{-0.47}$ instead of being constant. Using Eq. (21), we indeed predict a decay exponent $\xi = \frac{4}{3}(1 - 0.47) \approx 0.707$, in perfect agreement with the observed decay exponent. Note that the similarity with the value of the decay exponent observed in vortex dynamics is then purely incidental.

In the experiment [5], the authors obtained $\tau_{\text{merg.}} \sim t^{0.6}$, which strongly indicates that they had not yet reached the scaling regime, which is not too surprising as the experiment was performed on less than a time decade. As mentioned in section **II.B**, this should raise some doubts about the validity of the apparent exponent $\xi \approx 0.7$.

III. NUMERICAL RENORMALIZATION GROUP (RG)

A. Implementation of the numerical RG

In this section, we address the problem of performing long-time simulations allowing for low vortex density *and* total vortex area coverage. Direct simulations of Kirchhoff equations are doomed to failure since each evaluation of a vortex velocity involves the sum over N terms (see Eq. (4) and Eq. (5)). To access very low densities, one must therefore start out with a very large initial number of vortices, which results in a very slow early dynamics.

The idea of the new approach that we introduce in this section, is to work with a *constant* number of vortices in a reasonable range ($N \sim 20 - 100$), and progressively increase the domain size L by a procedure detailed below. For simplicity, we work with vortices of identical radii at all times and thus of equal circulation up to a sign. This is probably a reasonable approximation, as previous short-time simulations and experiments have shown that the radius and circulation distributions remain narrow at all times [9,16,22]. Therefore, the universal features of the dynamics are expected to survive. Moreover, keeping such constant distributions in time should minimize transient time effects due to the fact that the scaling distributions are not yet reached (although this problem is partly taken into account by the clever procedure introduced in [9]).

We thus consider N vortices of radius r and circulation $\Gamma = \pm\omega\pi r^2$ ($N/2$ vortices of each sign) in a box of initial linear size L , such that the initial density is $n_0 = N/L^2$. Periodic boundary conditions are considered and Kirchhoff equations of motion are adapted to this situation [8,9]. Compared to Eq. (4) and Eq. (5), the velocity induced by a vortex j on a vortex i is only significantly different for vortices at a distance of order L , so that the physics is not modified particularly for vortices at a typical distance L/\sqrt{N} or less.

Vortices do obey Kirchhoff dynamics until two like-sign vortices meet, *i.e.* their distance is less than $r_c = 2r$ (see the discussion of section **II.A**). Both vortices are merged, and all radii and circulations are updated to

$$r' = \left(\frac{N}{N-1}\right)^{\frac{1}{4}} r, \quad \Gamma' = \pm\omega\pi r'^2. \quad (22)$$

The density is updated accordingly:

$$n' = \frac{N-1}{N} n. \quad (23)$$

A new vortex of the same sign as the vortex which just disappeared is then introduced in the box at a random position and has radius r' and circulation Γ' . The number of vortices in the box is then restored to its initial value N . All the distances are then scaled by a factor $\left(\frac{N}{N-1}\right)^{1/2}$:

$$L' = \left(\frac{N}{N-1}\right)^{\frac{1}{2}} L, \quad \mathbf{r}'_i = \left(\frac{N}{N-1}\right)^{\frac{1}{2}} \mathbf{r}_i. \quad (24)$$

This renormalization procedure ensures that the new density takes the correct value

$$n' = \frac{N}{L'^2} = \frac{N-1}{N} \frac{N}{L^2} = \frac{N-1}{N} n, \quad (25)$$

and that the quantity $n'r'^4 = nr^4$ is conserved, ensuring the conservation of the energy per area unit. If N is large enough, one may expect that the introduction of a new uncorrelated vortex after each merging should not affect the dynamics, especially at large times for which the merging time is much larger than the mean free time. In this regime, the newly introduced vortex which has only a probability N^{-1} of being involved in the next collision has plenty of time to get “randomized” as $\tau_{\text{merg.}} \gg \tau$.

B. Numerical results

We have performed long-time RG simulations with $N = 10, 20, 40, 60, 80$ vortices, reaching final densities as low as $2 \times 10^{-4} n_0$. Except for the case $N = 10$ which seems to decay faster, the different density plots are essentially independent from the actual number of vortices involved in the RG (see fig. 1). The long-time decay exponent is estimated to be $\xi = 0.99 \pm 0.01$ significantly higher than the expected value $\xi \approx 0.7$ but still well below the naïve estimate $\xi = 4/3$ obtained in section II.C.

We have also measured the average mean square displacement of surviving vortices. The motion is found to be hyperdiffusive with a diffusion exponent ν consistent with the prediction of section II.C and [21]. Indeed, we find $\nu = 1.50 \pm 0.01$, to be compared with $\nu = 3/2$, admitting the value $\xi = 1$. This is illustrated in fig. 2. Note that according to section II.C.2, we thus predict a flight time distribution behaving as $P(\tau) \sim \tau^{-5/2}$, for large τ .

In the range $n/n_0 = 0.8 - 0.2$, corresponding to the range of density obtained in previous experiments [3–5] and simulations [6,9,13,16], we indeed obtain an apparent exponent of order $\xi \approx 0.7$. In fig. 3, we compare the direct simulations of [9,16] where vortices were allowed to develop a scaling radius distribution. After fitting an arbitrary time scale, it appears that our RG simulations are in good agreement with these previous works, although our RG simulations extend to almost three more decades in time.

We have also measured the mean square vortex velocity which is expected to behave as

$$\langle v^2 \rangle \sim n \Gamma^2 \ln \left(\frac{L(t)}{r(t)} \right) \sim \ln(t). \quad (26)$$

This behavior is confirmed by our RG numerical simulations as shown in fig. 4.

We have also performed RG simulations introducing a distance cut-off in Kirchhoff equations Eq. (4) and Eq. (5), replacing r_{ij}^2 by $(r_{ij}^2 + r^2)$. Indeed, although like-sign vortices cannot approach each other closer than a distance $2r$ (otherwise they merge), opposite-sign vortices can, which is quite unphysical as it generates very fast traveling dipoles. Introducing this cut-off results in a physical upper cut-off of order Γ/r for the maximum velocity of these dipoles. The number of vortices initially decays slightly more slowly, although the long-time decay exponent remains fully compatible with $\xi \approx 1$.

It is interesting to compare our results to new direct simulations where the radii and modulus of circulation are maintained equal for all surviving vortices. Even starting from $N = 2000$, it is hard to reach low densities in a reliable way. As exemplified in fig. 5, these direct simulations follow our RG calculations before decaying faster beyond a breaking time t_N , as the density approaches the minimum reachable density $n/n_0 = 2/N$. We observe that the breakdown occurs sooner for samples with a decreasing initial number of vortices. t_N is in fact of the order of the minimum time after which some samples had reached the minimum possible density (only 2 opposite vortices left). Still, fig. 5 lends credence to the claim that the large N limit finally reproduces the RG results. Note finally that for these direct simulations, the actual logarithmic correction in the mean square velocity behaves differently from that in the RG simulations as the box size L remains constant. In this case, it slowly decreases as

$$\langle v^2 \rangle \sim n\Gamma^2 \ln \left(\frac{L}{r(t)} \right) \sim \ln \left(\frac{t_*}{t} \right), \quad (27)$$

up to a time of order $t_* \sim t_N$. Note that this subdominant difference between RG and direct simulations could be responsible for a slight discrepancy in the apparent decay exponent observed in both kinds of simulations.

IV. MERGING TIME IN EFFECTIVE TWO-BODY AND THREE-BODY DYNAMICS

A. General form of the merging time

In this section, we are concerned with an alternative way of evaluating the merging time $\tau_{\text{merg.}}$ as a function of the physical parameters $n, r, \Gamma \dots$. On the basis of simple dimensional analysis, $\tau_{\text{merg.}}$ can be expected to be proportional to the mean free time τ multiplied by an arbitrary function of the only dimensionless parameter nr^2 . Expecting power-law behaviors for these quantities, a natural *ansatz* is

$$\tau_{\text{merg.}} \sim \frac{\tau}{(nr^2)^\alpha}, \quad (28)$$

where α is an exponent to be determined. Dropping logarithmic corrections in τ (see Eq. (13)), we obtain

$$\tau_{\text{merg.}} \sim (n\Gamma(nr^2)^\alpha)^{-1} \sim \omega^{-1}(nr^2)^{-(1+\alpha)}. \quad (29)$$

Imposing that $\tau_{\text{merg.}}$ must be proportional to the actual time (see section **II.C**), and using the scaling equations Eq. (8), we find the relation between the decay exponent ξ and α :

$$\xi = \frac{2}{1 + \alpha}. \quad (30)$$

Note that the naïve expression of $\tau_{\text{merg.}}$ obtained in section **II.C** can also be written in this form:

$$\tau_{\text{merg.}} \sim (nvr)^{-1} \sim \omega^{-1}(nr^2)^{-3/2}, \quad (31)$$

corresponding to $\alpha = 1/2$ and thus $\xi = 4/3$.

B. Theory of the effective two-body dynamics

We now consider the effective dynamics of two *nearby* like-sign vortices, assuming that the $(N - 2)$ other vortices are at a distance *at least of order* R . The velocity induced by the other vortices on one of these two vortices can be written as the sum of the velocity induced on the center of mass (at $\mathbf{r}_0 = (\mathbf{r}_1 + \mathbf{r}_2)/2$) plus a small correction:

$$v_{1x} = - \sum_{j \neq 1,2} \Gamma_j \frac{y_{1j}}{r_{1j}^2}, \quad (32)$$

$$= v_{0x} + \delta x_1 \sum_{j \neq 1,2} \Gamma_j \frac{x_{0j} y_{0j}}{r_{0j}^4} + \delta y_1 \sum_{j \neq 1,2} \Gamma_j \frac{y_{0j}^2 - x_{0j}^2}{r_{0j}^4}, \quad (33)$$

$$= v_{0x} + \delta x_1 \eta_a + \delta y_1 \eta_b, \quad (34)$$

where we have neglected other corrections involving higher powers of $\delta x_1 = x_1 - x_0$ and $\delta y_1 = y_1 - y_0$. After a straightforward calculation, we get a similar equation for v_{1y} :

$$v_{1y} = v_{0y} + \delta x_1 \eta_b - \delta y_1 \eta_a. \quad (35)$$

Note the antisymmetric structure of Eq. (34) and Eq. (35) resulting from the Hamiltonian nature of the dynamics.

We will now assume that v_{0x} , v_{0y} , η_a and η_b can be considered as random Gaussian variables. Their second moments are respectively

$$\langle v_{0x}^2 \rangle = \langle v_{0y}^2 \rangle = \frac{\langle v^2 \rangle}{2} \sim n\Gamma^2, \quad (36)$$

up to a logarithmic term (see section **II.C** and [16,11,21]), and

$$\langle \eta_a^2 \rangle = \langle \eta_b^2 \rangle = N\Gamma^2 \left\langle \frac{x^2 y^2}{r^8} \right\rangle \sim N\Gamma^2 \frac{1}{L^2} \int_R^L \frac{x^4}{x^8} dx \sim n^2 \Gamma^2. \quad (37)$$

We have used R as the lower cut-off since the other vortices were assumed to be at a distance at least of order R . Note that $\eta_{a,b}$ have the dimension of an inverse time and are simply of order $\tau^{-1} \sim n\Gamma$. It is natural to assume that $\eta_{a,b}$ have the same correlation time as the velocity, namely the mean free time τ .

Assuming that $v_{0,x,y}$ and $\eta_{a,b}$ are Gaussian noises of correlation time τ leads us to write a simplified effective Langevin equation describing the dynamics of these four quantities:

$$\frac{du}{dt} = -\frac{u}{\tau} + \frac{\langle u^2 \rangle}{\tau^{1/2}} w_u, \quad (38)$$

where $u = v_{0,x,y}, \eta_{a,b}$, and w_u are independent δ -correlated white noises. Such a Langevin equation was recently introduced to describe velocity fluctuations in [11], with reasonable success.

We are now ready to construct an effective two-body system in order to study the merging time. We consider two like-sign vortices of identical circulation in a square box of size R with periodic boundary conditions. These vortices are submitted to their mutual advection and to the effective noise induced by the other vortices at a distance greater than R . If we define $x = x_1 - x_2$, $y = y_1 - y_2$ and $d = \sqrt{x^2 + y^2}$, we get from Kirchhoff equations and Eq. (34) and Eq. (35)

$$\frac{dx}{dt} = -\Gamma \frac{y}{d^2} + x\eta_a + y\eta_b, \quad (39)$$

$$\frac{dy}{dt} = \Gamma \frac{x}{d^2} + x\eta_b - y\eta_a, \quad (40)$$

as the average induced velocity cancels out. After expressing time in units of τ ($t \rightarrow t/\tau$) and distance in units of R ($x \rightarrow x/R$, $y \rightarrow y/R$), and noting that $\Gamma \sim R^2/\tau$, we end up with a dimensionless equation of motion as anticipated in the previous subsection:

$$\frac{dx}{dt} = -\frac{y}{d^2} + x\eta_\alpha + y\eta_\beta, \quad (41)$$

$$\frac{dy}{dt} = \frac{x}{d^2} + x\eta_\beta - y\eta_\alpha, \quad (42)$$

where $\eta_{\alpha,\beta}$ are independent Langevin random variables, of unit mean square average and correlation time.

Both vortices are initially randomly placed in the unit box at a mutual distance $d > 0.4R$ and their relative distance evolves according to Eq. (41) and Eq. (42) until d becomes smaller than the scaled dimensionless parameter $d_c = 2r/R = 2\sqrt{nr^2}$, which defines the merging time. As anticipated above, the average merging time in units of τ can only be a function of this parameter d_c , leading to Eq. (28).

C. Absence of strictly two-body collisions

Numerical simulations of Eq. (41) and Eq. (42) lead to the following surprising result: both vortices remain at a relative distance greater than a constant d_{\min} which slightly depends on the actual numerical constants in Eq. (41) and Eq. (42) (to simplify, we have assumed the coefficients of $(x, y)/d^2$, $\langle \eta_{a,b}^2 \rangle$, and the correlation time of $\eta_{a,b}$ to be exactly equal to 1). A typical long-time trajectory is shown in fig. 6 and perfectly illustrates the absence of collisions when the vortex size is below a certain threshold. Note that if there were no noise due to the other vortices, both vortices would strictly remain at the same distance, hence producing a circular trajectory.

Of course, our result does not prove the absence of collision in the actual N -body system, but strongly suggests that the main assumption according to which all other vortices are at a distance greater than R prevents both test vortices from colliding.

Let us now give a physical interpretation of our result. If both test vortices were at the same point, their distance would not vary since the velocity induced by the other vortices would be exactly the same for both vortices. Thus, when they are close to each other, the effective induced noise is reduced linearly with their distance d as shown by Eq. (41) and Eq. (42). In addition, as vortices get closer to each other ($d \sim r$), their relative position describes a circle, moving at angular velocity of order

$$\Omega \sim v_r \times r^{-1} \sim \frac{\Gamma}{r} \times r^{-1} \sim \omega. \quad (43)$$

Because of this fast rotation, the effective fluctuation time of the noise, as seen in the moving frame, becomes $\omega^{-1} \ll \tau$ instead of τ . Hence, not only the driving noise is reduced due to the proximity of the test vortices, but it is also averaged out due to their fast rotation. Such a short effective fluctuation time was in fact introduced in [16]. Another way of interpreting the effect of the fast vortex rotation is to note that due to the large difference between the system natural frequency ω and that of the noise perturbation ($\omega' \sim \tau^{-1}$), the adiabatic theorem ensures that the effective perturbation is reduced by a factor of order $\exp(-C\omega\tau)$, where C is a constant of order unity [23].

Conversely, if both vortices start at a distance $d < d_{\min}$, this fast rotating pair remains stable for a very long time, probably infinite. Such pairs can thus only be destroyed by the direct interaction with a third vortex, and not solely by the background noise.

The results of this section suggest that strictly two-body interactions are not sufficient to generate collisions. It is thus natural to study the equivalent three-body problem, which is the subject of the next section.

D. Merging time of a three-body system

Using Eq. (34) and Eq. (35), we can generalize our preceding approach to the case of three test vortices submitted to the effective noise induced by far away vortices. For the first vortex, the effective equation of motion now reads

$$\frac{dx_1}{dt} = -\Gamma_2 \frac{y_{12}}{r_{12}^2} - \Gamma_3 \frac{y_{13}}{r_{13}^2} + \delta x_1 \eta_a + \delta y_1 \eta_b + v_{0x}, \quad (44)$$

$$\frac{dy_1}{dt} = \Gamma_2 \frac{x_{12}}{r_{12}^2} + \Gamma_3 \frac{x_{13}}{r_{13}^2} + \delta x_1 \eta_b - \delta y_1 \eta_a + v_{0y}, \quad (45)$$

with similar equations for the two other test vortices. As we are studying the merging time of like-sign vortices, we take vortex 1 and 2 to be of circulation $+\Gamma$, whereas vortex 3 is left unspecified, with circulation $\pm\Gamma$.

As in the preceding section, these effective equations of motion can be rescaled by expressing distances in units of R and times in units of τ . In these new units, a collision between vortices 1 and 2 occurs when the distance between them is less than the scaled dimensionless parameter $d_c = 2r/R$.

The sign of the third vortex plays a significant role. When it is the same as that of the other two, a phenomenon reminiscent of that which was found for two-body collisions occurs: vortices do not collide below a certain radius, at least during numerically observable times.

On the contrary, when this third vortex is of the opposite sign, we observe a smooth dependence of the merging time as a function of d_c , which is fully compatible with the functional form (see fig. 7)

$$\tau_{\text{merg.}} \sim \frac{\tau}{nr^2}, \quad (46)$$

that is $\alpha = 1$, and thus $\xi = 1$ using the results of section **IV.A**. This result is in agreement with our RG calculation, for which we also found $\xi \approx 1$. Note that for r/R large, corresponding to the early stage of the actual dynamics, the apparent value of α is of order $\alpha \sim 2$, which is compatible with an apparent decay exponent in the range $\xi \sim 0.6 - 0.7$ (see the inset of fig. 7).

V. PHYSICAL PICTURE

The present study strongly suggests that for small surface coverage ($r/R \ll 1$), the relevant collision mechanism involves three vortices, one having an opposite circulation from the other two. A naïve picture would be that of a $(+\Gamma, -\Gamma)$ dipole moving at the typical velocity Γ/r encountering an isolated vortex of any sign. The importance of these fast traveling pairs was already suggested in [8,11]. It is likely that the three-body collision processes need not to strictly occur in the simple way described above, although this does provide an evocative physical picture from which to construct an effective kinetic theory.

Following the interpretation presented above, the collision rate is

$$\frac{dn}{dt} \sim -n_{\text{dip.}} \times nv_{\text{dip.}}r, \quad (47)$$

where $n_{\text{dip.}}$ and $v_{\text{dip.}}$ are the dipole density and typical velocity, and the last term is the probability per unit time for a dipole to collide with an isolated vortex. In a simple mean-field approach, dipoles of typical size r are formed with density

$$n_{\text{dip.}} \sim n \times nr^2, \quad (48)$$

their velocity being of order $v_{\text{dip.}} \sim \Gamma/r$. Finally, we obtain

$$\frac{dn}{dt} \sim -n \times n^2 r^2 \Gamma, \quad (49)$$

which corresponds to a merging time

$$\tau_{\text{merg.}} \sim (n\Gamma \times nr^2)^{-1} \sim \frac{\tau}{nr^2}, \quad (50)$$

which in the language of section **II.C** leads to $\alpha = 1$, and then to $\xi = 1$ (up to logarithmic corrections).

This simple interpretation reconciles the paradoxical observation that although vortices are *hyperdiffusive* (see section **II.C.1** and **III.B**) the observed decay exponent ξ is *lower* than that found for diffusive aggregation [16,24,25] (see also section **II.C.2**). The dynamics is slowed down by the requirement of three close vortices for an actual merging to occur, at least for small area coverage. Note that using Eq. (50) and energy conservation, we can also write

$$\tau_{\text{merg.}} \sim \frac{\omega L^2}{nE}. \quad (51)$$

This relation is particularly well obeyed in the experiment described in [5], LHS and RHS terms being respectively

$$\tau_{\text{merg.}} \sim t^{0.57 \pm 0.12}, \quad \text{and} \quad \frac{\omega L^2}{nE} \sim \frac{t^{-0.15 \pm 0.04}}{t^{-0.70 \pm 0.1}} \sim \sim t^{0.55 \pm 0.14}. \quad (52)$$

Thus, although $\tau_{\text{merg.}}$ does not behave linearly with time in the experiment, which is probably due to the fact that the scaling regime was not reached, all the relations found between physical quantities ($D \sim n^{-1/2}$, $\nu = 1 + \xi/2$ and $\mu = 3 - \xi/2$ in section **II.C**, and the above relation Eq. (51)) are fully consistent with our kinetic theory.

Note that Eq. (49) was obtained by Pomeau [15] and by one of us [16], but with the use of highly questionable physical arguments. In [15], the kinetic equation was written in the form

$$\tau \frac{dn}{dt} \sim -n \times nr^2, \quad (53)$$

by arguing that after a time of order τ the collision probability is simply the geometrical overlapping probability nr^2 , although a cross-section argument is definitely required (see section **II.C**). This argument boils down to the assumption that after a time τ , the vortex positions can be considered to be randomly generated, and collisions happen if two vortices overlap. In [16], inspired by the theory of diffusive aggregation [24,25], the kinetic equation was written in the form

$$\frac{dn}{dt} \sim -Dn^2, \quad (54)$$

but with an incorrect expression for the diffusion coefficient D (found constant in [16]). In [16], the fact that $\langle v^2 \rangle$ is essentially constant was correctly used, but the fluctuation time was taken as ω^{-1} instead of τ . As we have seen in section **IV.C**, it happens that just before a collision, the effective fluctuation time in fact becomes equal to ω^{-1} , which makes the agreement of Eq. (54) with Eq. (49) rather incidental.

VI. CONCLUSION

In this paper, we have introduced a numerical RG procedure which permits very long-time simulations of the vortex Kirchhoff dynamics in a two-dimensional decaying fluid. Although we recover a short-time regime compatible with a decay exponent of order $\xi \approx 0.7$

when the vortex surface coverage is still large and $n/n_0 \gtrsim 0.2$, we ultimately find a long-time asymptotic decay with $\xi \approx 1$. None of these results can be explained by the simple kinetic theory of section **II.C** based on the occurrence of two-body collisions which predicts $\xi = 4/3$. The failure of this “naïve” kinetic theory could be explained by our claim that strictly two-body collisions are irrelevant for small enough vortex surface coverage (section **IV.C**). For collision processes involving two like-sign vortices and a third opposite-sign vortex, we found an average merging time $\tau_{\text{merg.}} \sim \tau/(nr^2)$, fully consistent with a decay exponent $\xi = 1$ (section **IV.C**). A simple kinetic theory based on this collision mechanism also leads to $\xi = 1$ and predicts that $\tau_{\text{merg.}} \sim \frac{\omega L^2}{nE}$ in agreement with the experiment described in [5]. Our prediction [21] that the mean square displacement of surviving vortices goes as $\langle x^2 \rangle \sim t^{1+\xi/2}$ is in good agreement with our RG simulations and with experiments. Moreover, the exponent describing the decay of the flight time distribution is related to ξ by $\mu = 3-\xi/2$, in perfect agreement with experiment.

Our work has so far been limited to the study of the dynamics of a population of vortices *having the same radii* at all times. However, it is important to address the question of the possible dependence of the decay exponent ξ on the form of the radius distribution and/or the initial conditions [26], in order to verify its possible universality. Thus, it is a motivating challenge to generalize our RG approach to the case of a polydisperse assembly of vortices. A crucial point would be to correctly specify the radius of the new vortex reinjected after each merging event. This and the study of the effective three-body dynamics of different size/circulation vortices should be the subject of a future study [27].

ACKNOWLEDGMENTS

We are grateful to Jane Basson for useful comments on the manuscript, and to Sidney Redner and Dima Shepelyansky for fruitful discussions. We also thank Bérengère Dubrulle for her interest in this work.

REFERENCES

- [1] C.F. Driscoll and K.S. Fine, *Phys. Fluids. B* **2**, 1359 (1990).
- [2] P.-H. Chavanis, J. Sommeria and R. Robert, *Astrophys. J.* **471**, 385 (1996); P.-H. Chavanis, *Annals N.Y. Acad. Sci.* **867**, 120 (1998).
- [3] P. Tabeling, S. Burkhart, O. Cardoso and H. Willaime, *Phys. Rev. Lett.* **67**, 3772 (1991).
- [4] O. Cardoso, D. Marteau and P. Tabeling, *Phys. Rev. E* **49**, 454 (1994).
- [5] A.E. Hansen, D. Marteau and P. Tabeling, *Phys. Rev. E* **58**, 7261 (1998).
- [6] J.C. McWilliams, *J. Fluid. Mech.* **146**, 21 (1984).
- [7] G.F. Carnevale, J.C. McWilliams, Y. Pomeau, J.B. Weiss and W.R. Young, *Phys. Rev. Lett.* **66**, 2735 (1991).
- [8] J.B. Weiss and J.C. McWilliams, *Phys. Fluids A* **3**, 835 (1991).
- [9] J.B. Weiss and J.C. McWilliams, *Phys. Fluids A* **5**, 608 (1993).
- [10] A. Siegel and J.B. Weiss, *Phys. Fluids A* **9**, 1988 (1997).
- [11] J.B. Weiss, A. Provenzale and J.C. McWilliams, *Phys. Fluids A* **10**, 1929 (1998).
- [12] R. Benzi, S. Patarnello and P. Santangelo, *Europhys. Lett.* **3**, 811 (1987).
- [13] R. Benzi, M. Colella, M. Briscoloni and P. Santangelo, *Phys. Fluids A* **4**, 1036 (1992).
- [14] G. Riccardi, R. Piva and R. Benzi, *Phys. Fluids* **7**, 3091 (1995).
- [15] Y. Pomeau, *J. Plasm. Phys.* **56**, 3 (1996); **56**, 407 (1996). See also, Y. Pomeau, in *Turbulence: A Tentative Dictionary*, Eds. P. Tabeling and O. Cardoso (Plenum Press, NY 1995); Communication at the conference *Turbulencia*, Ed. M.G. Velarde (Aguadulce, Spain 1993).
- [16] C. Sire, *J. Techn. Phys.* **37**, 563 (1996).
- [17] E.A. Novikov, *Sov. Phys. JETP* **41** (5), 937 (1975).
- [18] G. Kirchhoff, in *Lectures in Mathematical Physics, Mechanics* (Teubner, Leipzig, 1877).
- [19] M.V. Melander, N.J. Zabusky and J.C. McWilliams, *J. Fluid. Mech.* **195**, 303 (1988).
- [20] G.K. Batchelor, *Phys. Fluids Suppl. II* **12**, 233 (1969).
- [21] P.-H. Chavanis and C. Sire, submitted to *Phys. Rev. E* (1999), cond-mat/9911032.
- [22] E. Trizac, *Europhys. Lett.* **43**, 671 (1998); Thèse de Doctorat de l'École Normale Supérieure de Lyon (1997).
- [23] L. Landau and E. Lifchitz, *Cours de Mécanique* (Editions Mir, Moscou, 1984).
- [24] H. Takayasu, M. Takayasu, A. Provata and G. Huber, *J. Stat. Phys.* **65**, 725 (1991).
- [25] S.N. Majumdar and C. Sire, *Phys. Rev. Lett.* **71**, 3729 (1993).
- [26] X. He, in *Advances in Turbulence VI*, edited by S. Gavrilakis et al. (Kluwer, Dordrecht, 1996), p. 277.
- [27] C. Sire and P.-H. Chavanis, in preparation.

FIGURES

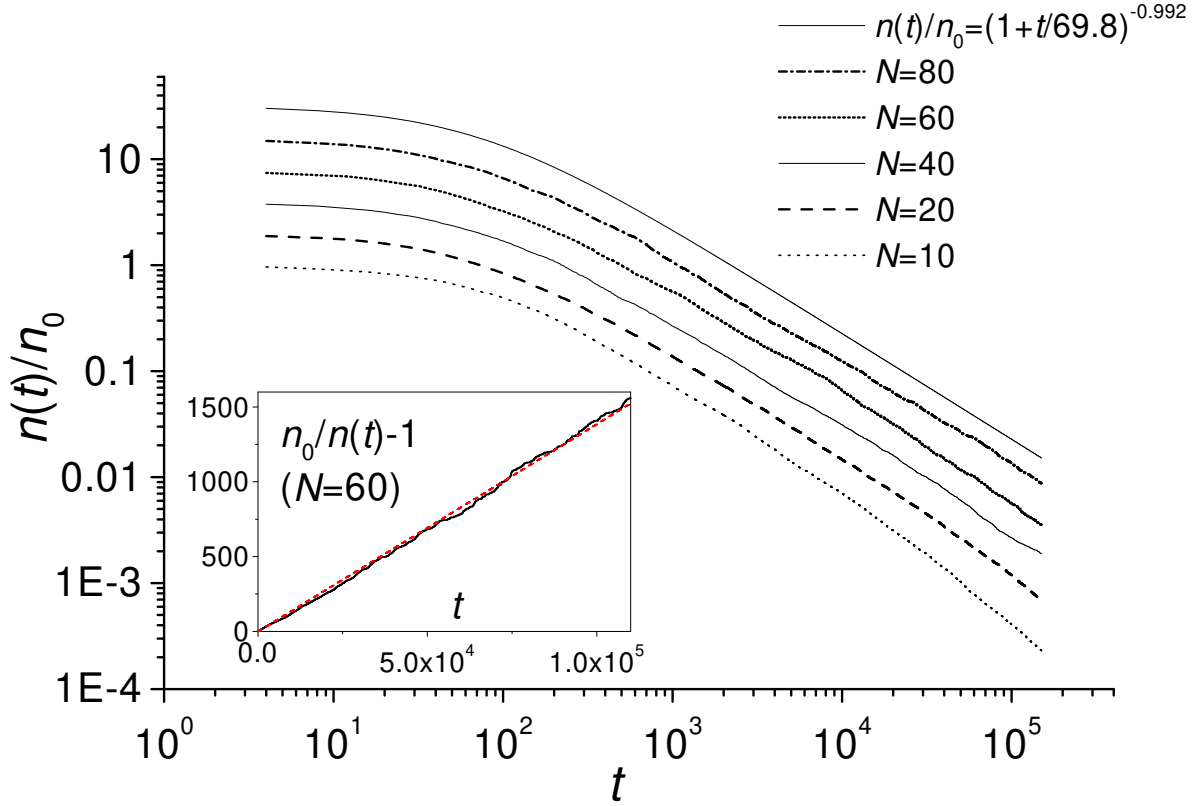


FIG. 1. Numerical RG simulations for $N = 10, 20, 40, 60, 80$ (resp. 250,150,30,20,10 samples) and the best fit of the $N = 20 - 80$ curves to the functional form $n(t)/n_0 = (1 + t/t_0)^{-\xi}$ (with $\xi = 0.992$ and $t_0 = 69.8$). For clarity, the curves have been offset by an arbitrary factor 2. The time t is expressed in units of ω^{-1} and the initial total area coverage is 10%, like for most simulations presented in this paper. The inset shows that $n_0/n(t) - 1$ is reasonably linear with time ($N = 60$), which is consistent with an exponent $\xi \approx 1$.

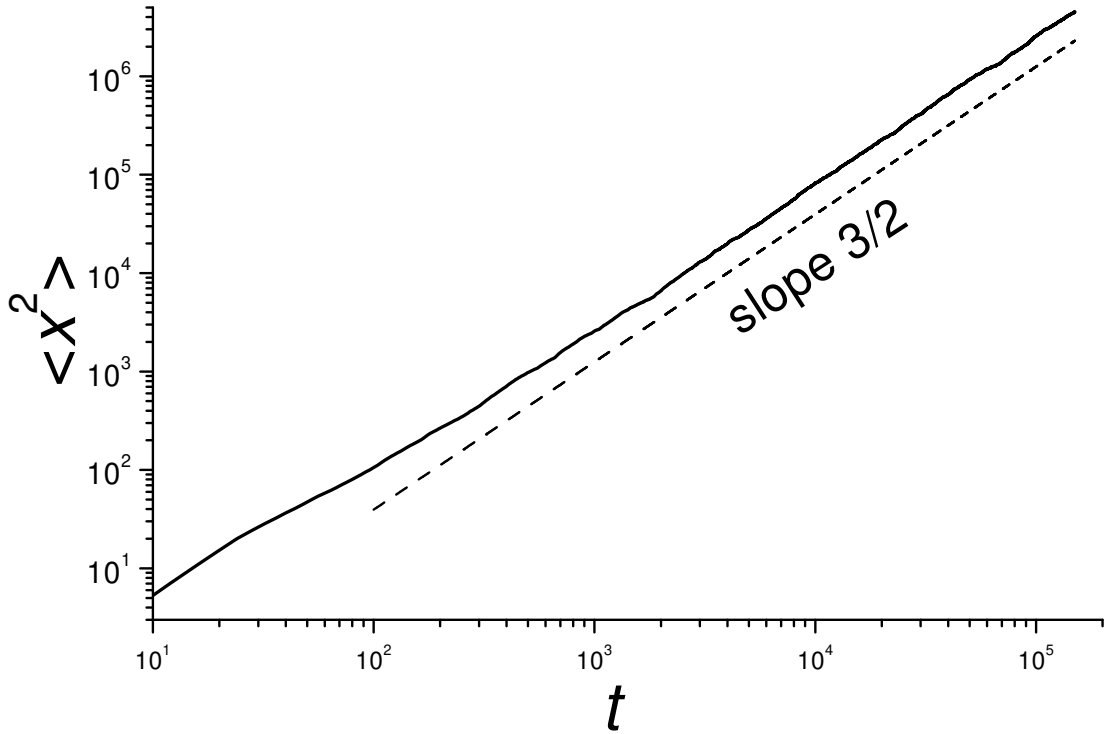


FIG. 2. Mean square displacement of surviving vortices as measured in $N = 40$ RG simulations. $\langle x^2 \rangle \sim t^\nu$, with $\nu = 1.50 \pm 0.01$, in perfect agreement with our prediction $\nu = 1 + \xi/2$ of Eq. (15), when taking $\xi = 1$.

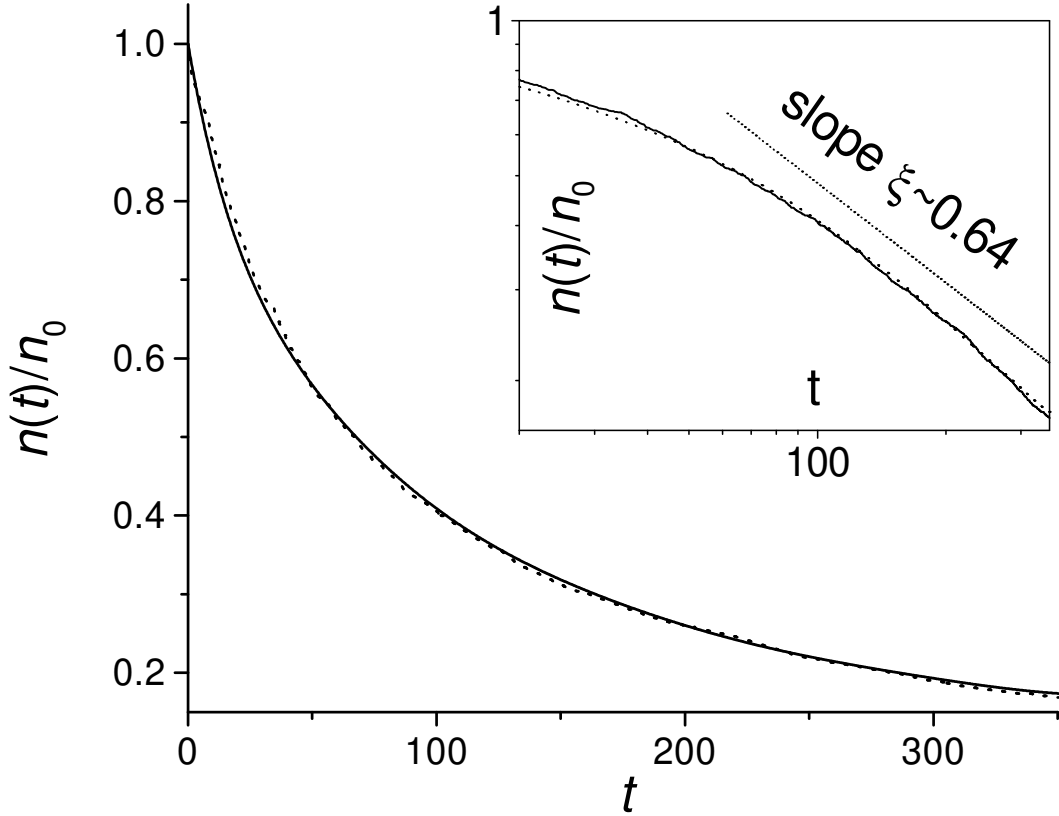


FIG. 3. We compare short time RG simulations (dashed curves, $N = 60$, 20 samples) with previous direct simulations including a polydisperse population of vortices (for which the time unit has been scaled to that of the RG simulations). The agreement is good and the apparent decay exponent is of order $\xi \approx 0.64$ (extrapolated to $\xi \sim 0.72 - 0.75$). However, the data display a strong curvature in a log-log plot (see inset).

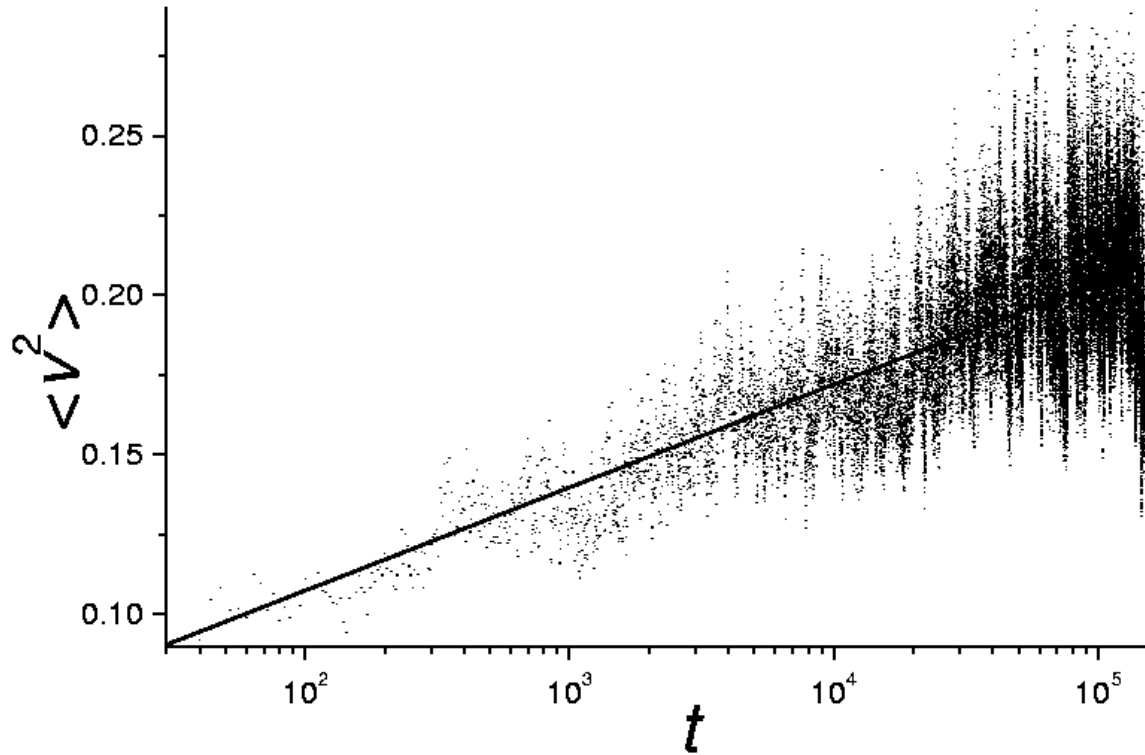


FIG. 4. The plot of $\langle v^2 \rangle(t)$ (RG simulations with $N = 80$; 10 samples; sampling time $\Delta t = 4\omega^{-1}$, with no time averaging) displays a slow variation of this quantity fully compatible with the logarithmic correction obtained in Eq. (26). The thick line is a log-linear fit of the scatter plot.

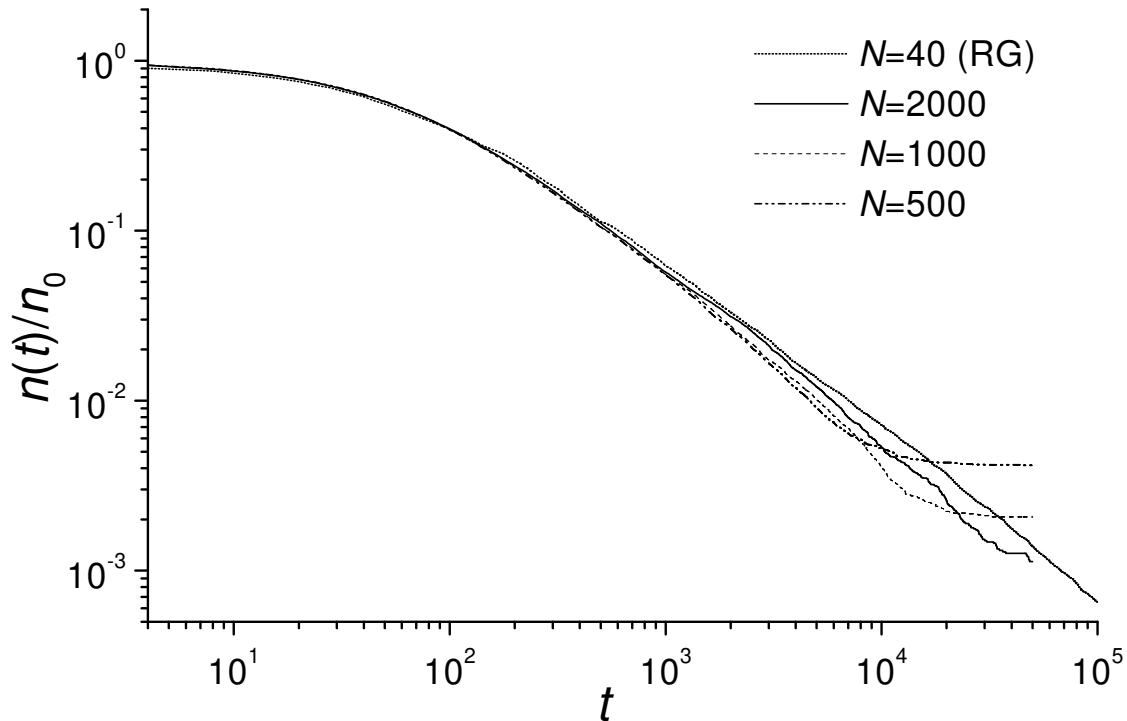


FIG. 5. Direct simulations maintaining all radii equal ($N = 500, 1000, 2000$) are compared to RG simulations ($N = 40$). The saturation to the minimum reachable density $n/n_0 = 2/N$ is clearly seen. However, the direct simulations follow the RG simulations on a longer time domain as N increases, up to a time t_N for which some samples have already reached the minimum density. The long time apparent exponent for $N = 2000$ is of order $\xi \approx 1.1$.

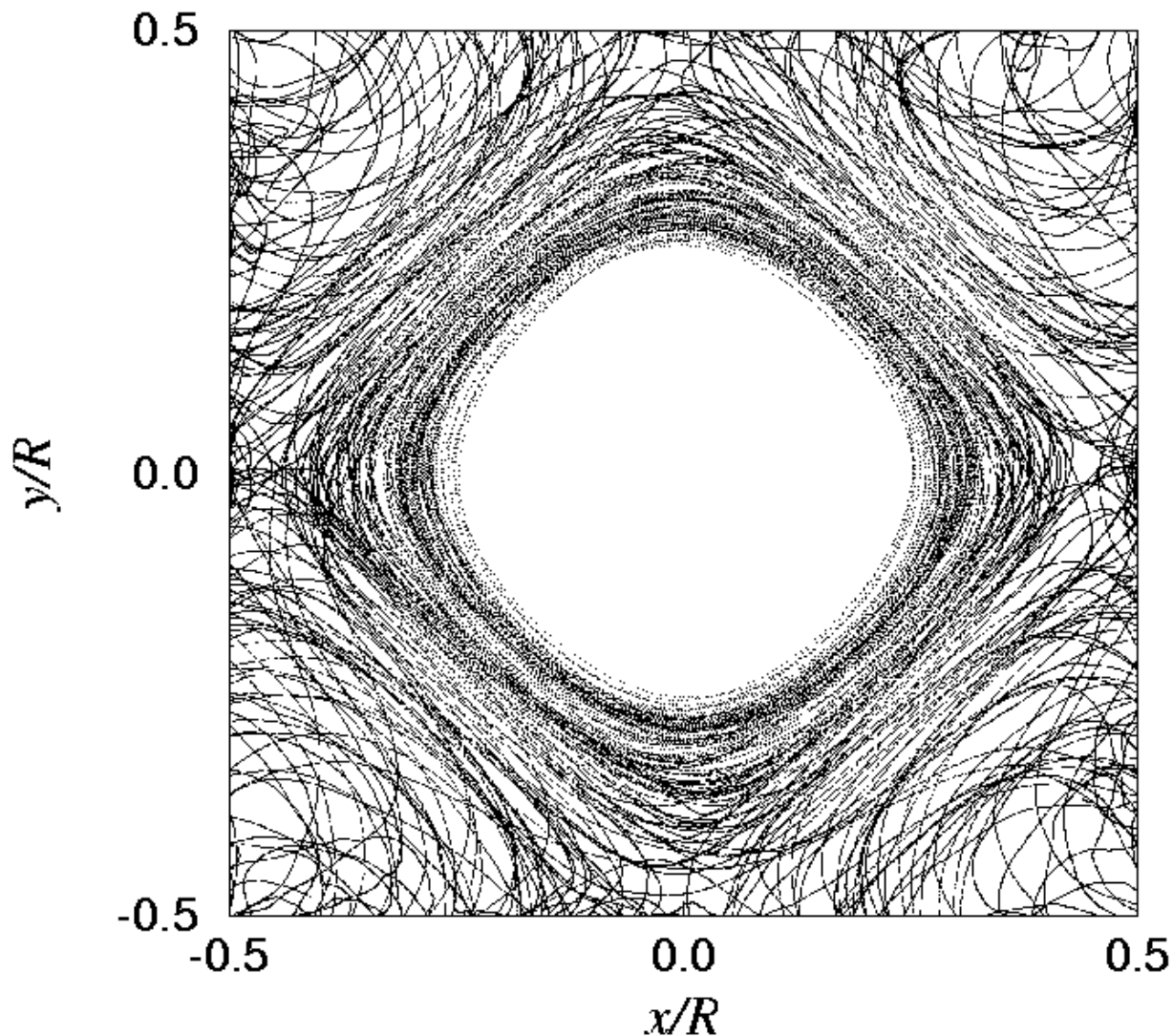


FIG. 6. We show a typical long-time relative trajectory within the effective two-body dynamics of section **IV.B**. For clarity, the final time is only $t_{\text{end}} = 200 \omega^{-1}$, although we have checked that the vortices never reach a distance less than $d_{\text{min}} \approx 0.24R$, up to $t_{\text{end}} \sim 10^5 \omega^{-1}$. The anisotropy of the (square-like) trajectory is due to the use of a Kirchhoff interaction adapted to periodic boundary conditions. As the distance d between vortices always remains of order R , these effects are visible, although they should disappear when $d \ll R$ (see discussion of section **III.A**). Still, note that when vortices are close to each other, their relative quasi-circular trajectory is not really affected by the noise due to other vortices, as explained in section **IV.C**.

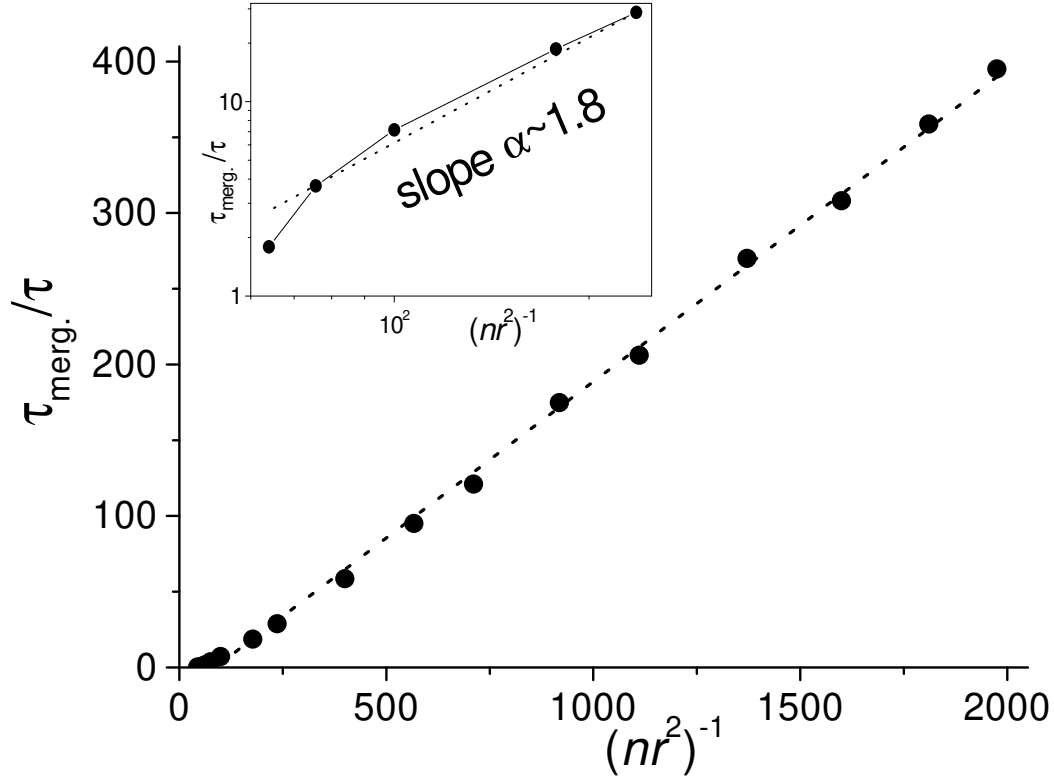


FIG. 7. We plot the average merging time $\tau_{\text{merg.}}$ in units of the mean free time as a function of the dimensionless parameter $(R/r)^2 = (nr^2)^{-1}$, as obtained within the effective three-body dynamics of section IV.D. We find a good linear behavior for small enough surface coverage. As explained in the text, this is consistent with a decay exponent $\xi = 1$. For large surface coverage (see inset), a log-log plot leads to an apparent exponent $\alpha \sim 1.8$, which is compatible with a decay exponent $\xi \sim 0.7$, in the language of section IV.A.